Boron Nitride Monolayers

DOI: 10.1002/anie.201003012

Formation of Boron-Based Films and Boron Nitride Layers by CVD of a Boron Ester**

Hermann Sachdev, Frank Müller, and Stefan Hüfner*

Monolayers of films of three-coordinate boron nitride (boronitrene layers)[1] resemble the BN analogues of graphene and can be deposited from borazine ($B_3N_3H_6$). However borazine is a very inconvenient compound both in terms of its synthesis by thermal cleavage of amineborane (H_3B-NH_3) and its stability.[2,3] The formation of a highly regular self-assembled nanostructure with a periodicity of 3.22 nm based on a boronitrene layer on Rh(111) ("NanoMesh") by chemical vapor deposition (CVD) of borazine was described by Corso et al.[4] and structural aspects of boronitrene layers were subsequently modeled.[5] Boronitrene layers resemble two-dimensional quantum barriers with a polar surface[6] and act as templates for trapping atoms or molecules.[7,8] Comparable effects have been reported for the self-assembly of supramolecular structures on graphene.[9] A variation of the lattice mismatch between the BN lattice and the substrate lattice offers the possibility to tune the shape and superstructures of the boronitrene nanostructures,[10–15] and sp^2-type boron nitride layers can act as insulating barriers on metal substrates and be used for the development of new electronic devices.[16] Studying the formation of hexagonal boron nitride (h-BN) from molecular precursors on transition-metal surfaces is of general interest to understand the nucleation and crystal growth of h-BN, which is a solid of high structural anisotropy. The chemical aspects of the BN formation are important for the syntheses of different BN modifications by CVD and physical vapor deposition (PVD)[17–19] and by high-pressure–high-temperature methods.[20–22] There are many reports regarding CVD concepts, where volatile molecular precursors contain structural motifs or subunits from which the solid material is to be built up. It was generally assumed that providing the structural subunits of the final product in the volatile species would enable a more facile formation of the desired solid material through the pre-existing connectivity of atoms, which would not need to be restructured during the growth of the solid. Borazine ($B_3N_3H_6$), containing a structural subunit of a six membered B_3N_3- ring system also present in a sp^2-type BN layer, was therefore considered as a suitable candidate for the CVD of sp^2-type BN phases.[1,4,7,8,10–15]

However, in a previous study it was shown that borazine is not a pre-requirement for the formation of a boronitrene layer, since the boronitrene layer can be reversibly formed from intermediate boron oxide species by nitrification with ammonia.[1] That study revealed that the nature of the molecular precursor has no influence on the nature of the BN film formed for the reported route. This feature is an important aspect regarding the use and limitations of single-source precursors for the deposition of three- or four-coordinate BN systems. Therefore, the search for suitable substitutes for borazine, which is highly reactive and easily decomposing material, was directed towards precursors which might lead to the formation of a boron oxide type layer, from which a BN monolayer can be generated by nitrification.

Boron–oxygen bonds are very stable (bond enthalpy for a B–O bond: 463 kJ mol^{-1}, boron oxide: $\Delta H_F =$ 1273.6 kJ mol^{-1}). Thus, $(MeO)_3B$ might serve as a CVD precursor leading directly to BO_x-films. Herein, this new route to BN monolayers (Figure 1) is discussed in chemical aspects along with the corresponding X-ray photoelectron

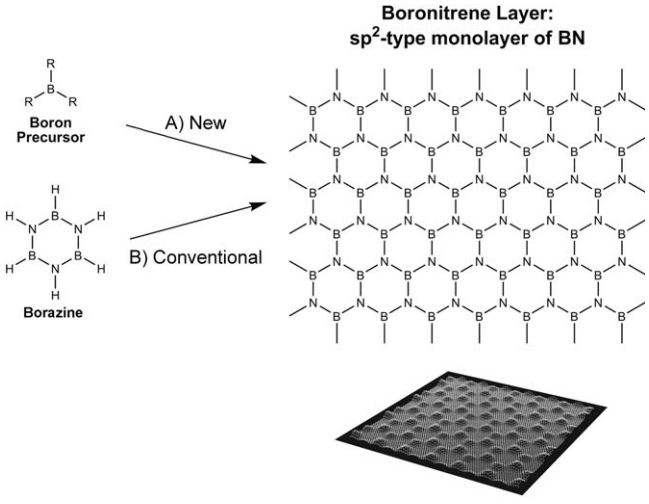

Figure 1. A) New route to boronitrene films: the layer is built up by selective chemical reactions from a boron source. B) Conventional route to boronitrene films: CVD of borazine. Right: Connectivity of a graphene-like BN layer and model of the topology of a BN monolayer in Rh(111) according to Ref. [5].

[*] Priv.-Doz. Dr. H. Sachdev[+]
Allgemeine und Anorganische Chemie FR 8.1
Universität des Saarlandes
Postfach 151150, 66041 Saarbrücken (Germany)
E-mail: h.sachdev@mx.uni-saarland.de
Dr. F. Müller, Prof. Dr. S. Hüfner
Experimentalphysik, Naturwissenschaftlich-Technische Fakultät II – Physik und Mechatronik, Universität des Saarlandes
66041 Saarbrücken (Germany)
[+] Current address: Max Planck Institute for Polymer Research
Ackermannweg 10, 55128 Mainz
E-mail: sachdev@mpip-mainz.mpg.de

[**] We gratefully acknowledge the financial support from the European Union under contract no. NMP4-CT-2004-013817 (Specific Targeted Research Project "Nanomesh") and M. Schreck and S. Gsell, University of Augsburg, for the provision of substrates.
CVD = chemical vapor deposition.

spectroscopy (XPS), X-ray photoelectron diffraction (XPD), and low-energy electron diffraction (LEED) data. Physical aspects, such as surface structures, are listed in Ref. [24].

The new approach is summarized as follows: CVD in ultrahigh vacuum of $(MeO)_3B$ was performed on a Rh(111) multilayer substrate (a silicon-based Rh(111)/YSZ/Si multilayer substrate[23]) and led to the formation of a boride type layer. Exposure of the boride type layer to oxygen gave a fully oxidized boron species on the substrate, and in analogy to a previous experiment,[1] exposure of this new BO_x epilayer to ammonia resulted in the formation of a superstructured boronitrene layer. A direct treatment of the boride type layer with ammonia gives a BN film with boron and carbon still present.

The XPS spectra of the films are shown in Figure 2 for C1s, O1s, N1s, and B1s, and relative intensities of detectable

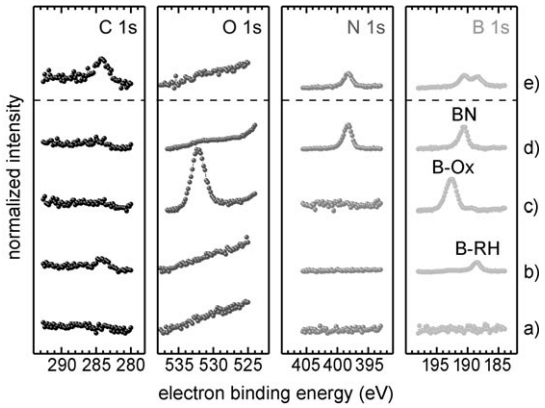

Figure 2. XPS signals of the films. XPS detail spectra (C1s, O1s, N1s, B1s; $Al_{K\alpha}$, $h\nu = 1486.6$ eV): a) clean Rh(111)/YSZ/Si multilayer substrate;[23] b) CVD of $(MeO)_3B$ (150 L $(MeO)_3B$ at 800 K), formation of a Rh-boride phase; c) oxidation of the Rh-boride phase from (b) (925 L O_2 at 900 K), indicating the presence of B-O-(H) species on the surface with a B:O ratio of 1:2; d) addition of ammonia (850 L NH_3 at 900 K) to the BO_x phase from (c), formation of BN (ca. 1:1), no oxygen present; e) direct nitrification of a Rh-boride film obtained from CVD of $(MeO)_3B$ in (b), with 1600 L NH_3 at 900 K.

signals are discussed. On the surface of the Rh(111) multilayer substrate (Figure 2a), no oxygen is detectable, there are only some ubiquitous traces of carbon (relative intensities: Rh:C ca. 0.98:0.02). The corresponding LEED profile (Figure 3a) reveals a well ordered Rh(111) surface. Deposition of 150 L $(MeO)_3B$ at 800 K leads to a film with no significant amount of oxygen according to the corresponding XPS signals (Figure 2b). The observed shift for the B1s signal at approximately 188.0 eV implies the formation of a boride type species[25] as well as some carbon (relative intensities: Rh:B:C ca. 0.90:0.05:0.05). The corresponding LEED profile (Figure 3b) reveals mainly an intensity for the (00) spot while the (10) spot is strongly decreased, but no additional peaks appear. This indicates a less ordered Rh(111) surface owing to lattice defects caused by the embedding of heteroatoms.

The results indicate that $(MeO)_3B$ must have been fragmented during CVD into species mainly delivering boron to the substrate and species containing oxygen and

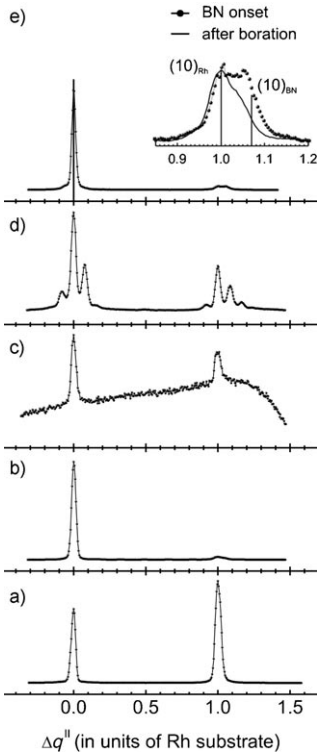

Figure 3. LEED profiles of the substrate and films. Intensity plots of the LEED profiles along the $[\bar{1}\bar{1}2]$ direction with diffraction patterns of the first order peaks. a) clean Rh(111)/YSZ/Si multilayer substrate;[23] b) CVD of $(MeO)_3B$ (150 L $(MeO)_3B$ at 800 K) formation of a Rh-boride phase as indicated by XPS; c) oxidation of the Rh-boride phase from (b) (925 L O_2 at 900 K) resulting in an unstructured, glassy film with a B:O ratio of 1:2 as found by XPS; d) addition of ammonia (850 L NH_3 at 900 K) to the BO_x phase from (c), formation of a highly ordered 14×14 BN/13×13 Rh (111)/YSZ/Si superstructure as described in Refs. [1, 24] (B:N ca. 1:1 as shown by XPS); e) direct nitrification of a Rh-boride film obtained from CVD of $(MeO)_3B$ in (b), with 1600 L NH_3 at 900 K indicates only formation of small BN domains. Inset the differences between the (01) spots in (b) and (e).

carbon. The film displays an XPS signal (for B1s ca. 188 eV) comparable to other transition-metal borides,[25] indicating a lowering of the formal oxidation state of boron from +3 in $(MeO)_3B$ to almost zero in the boride-type film. The amount of carbon present in the film equals the amount of boron for the first few nanometers, based on the surface sensitivity of the XPS analysis. Carbon contaminations can accumulate during UHV experiments (e.g. background pressure) in the same order of magnitude as reported herein. Even if the presence of carbon is fully attributed to cleavage products of the precursor, the observed amount would then formally be around 33% of the total amount of carbon that could be delivered by $(MeO)_3B$ [without considering carbon present on the substrate before decomposition (Figure 2a, Rh:C ca. 0.98:0.02), which would rescale this number to approximately 16%].

Reactions of primarily formed boron-oxygen species with carbon-hydrogen species resulting from the cleavage of $(MeO)_3B$ cannot be considered as being mainly responsible for boron formation, since B–O species are not significantly detectable by XPS on the Rh(111) substrate after CVD of

$(MeO)_3B$. In any case, the amount of carbon is far less than expected from the total intake resulting from $(MeO)_3B$ and the decay is highly selective as indicated by XPS (no significant O1s XPS intensity, no significant B1s XPS intensity in the range of BO_x species). Therefore, the results give rise to an interpretation of an unprecedented decay of $(MeO)_3B$ by CVD on Rh(111).

After CVD of $(MeO)_3B$, the corresponding LEED pattern still indicates the presence of a Rh(111) lattice structure, but with a less degree of ordering (Figure 3b). Patterns resulting from a distinct new structure were not detected. The XPD data of the boride type film obtained within the $[\bar{1}\bar{1}2]$–[111]–$[11\bar{2}]$ symmetry plane (Figure 4)[24]

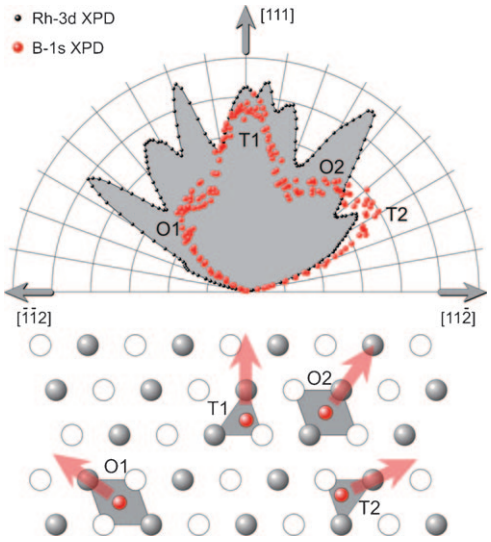

Figure 4. XPD of the boride phase obtained by CVD of $(MeO)_3B$: For the clean Rh(111) surface and after the deposition of $(MeO)_3B$, the angular distribution of the Rh-3d scattering is nearly the same, except a slight attenuation of the overall Rh-3d intensity after the deposition. Therefore, a dilute distribution of boron within the Rh lattice is expected and B–B scattering can be neglected in a first approximation. While the intensity distribution of the Rh-3d electrons exhibits all angular features that can be assigned to the main forward-scattering directions within the $[\bar{1}\bar{1}2]$–[111] and [111]–$[11\bar{2}]$ sectors, the B-1s intensity displays a significant asymmetry within these sectors, which correlates with the direction of tetrahedral interstitials (T1 and T2) of the Rh lattice. The B1s XPD data interestingly display nearly no anisotropy along directions for a regular octahedron (O1) or a distorted octahedron (O2) of the Rh lattice.[24]

shows an anisotropy of the B1s intensity, especially along the [111] direction. The observed B1s intensity modulations are caused by forward scattering and therefore indicate that boron is embedded in the Rh(111) substrate and not deposited on top. Intensity maxima are observed in directions which formally correlate with tetrahedral interstitials (T1, T2 in Figure 4) rather than octahedral interstitials (O1, O2 in Figure 4) of the Rh(111) substrate lattice. The strong forward scattering along the [111] direction indicates the presence of a Rh atom above a boron atom in the same direction as the tetrahedral interstitials (T1,T2) of the Rh(111) substrate. Regarding the coordination of boron in transition-metal borides, boron generally adopts high coordination numbers in transition-metal borides, as for example, observed in Refs. [26,27]. The decomposition of $(MeO)_3B$ was carried out at significantly lower Rh substrate temperatures as usually used for solid-state boride syntheses, and boron incorporation into a substrate by a CVD reaction may be governed kinetically before formation of a thermodynamically stable phase of distinct stoichiometry takes place, which may be further clarified by annealing experiments.

Exposure of the Rh boride-type film to a total of 925 L of O_2 at 900 K, resulted in the signal of the boride-type species at 188 eV vanishing and the formation of a boron oxygen species (XPS Figure 2c: B1s ca. 193 eV; Rh:B:O:C ca. 0.53:0.15:0.31:0.01; note: B:O ratio ca.1:2). All traces of carbon vanished (compare Figure 2b and c). Thus, carbon (irrespective of its origin) is removed almost completely by oxidation. The oxidation of carbon which can proceed faster than that of boron because of formation of volatile species (CO, CO_2).

Traces of boron may remain in the substrate presumably as a result of the oxidation kinetics being hindered in the newly formed BO_x film, preventing a further reaction. The observed B:O ratio of 1:2 is similar to the stoichiometry of a film obtained by oxidation of a boronitrene film and attributed to the formation of metaboric acid.[1] Since the present experimental setup does not allow the detection of hydrogen, the presence of metaboric acid can not explicitly be demonstrated, but gas impurities, background composition, and the precursor can be considered as ubiquitous sources of hydrogen. After precursor fragmentation, hydrogen may also be reversibly absorbed at, or embedded in, the substrate similar to boron and carbon. Therefore, the formation of metaboric acid with the experimentally observed B:O ratio of 1:2 is feasible during oxidation, which it should be possible to clarify subsequently by in situ IR or Raman spectroscopy or electron energy-loss spectroscopy (EELS). The LEED profile along the $[\bar{1}\bar{1}2]$ direction (Figure 3c), does not indicate the formation of an ordered epilayer. The damping of the (00) and (01) substrate spots and the enhanced background intensity give evidence for the formation of a disordered, glass-like surface structure of the newly formed B–O species, which would be in accordance with the properties of metaboric acid. Clearly the new procedure allows access to a boron–oxygen film on an Rh(111) substrate in a new way.

Exposure to ammonia (850 L at 900 K) led to a complete conversion of the BO_x film into a superstructured boronitrene layer on Rh(111).

An XPS analysis (Figure 2d: B1s 190.6 eV, N1s 398.2 eV; ratio for Rh:B:N:C approximately 0.74:0.13:0.12:0.01; B:N ratio ca. 1:1) indicates B1s and N1s signals, which are fully comparable to those of described boronitrene layers.[1] A LEED profile along the $[\bar{1}\bar{1}2]$ direction (Figure 3d) reveals the formation of an ordered superstructure of the BN layer as shown by the appearance of additional non-integral spots that can be attributed to a 14×14 BN/13×13 Rh(111) superstructure on the multilayer substrate.[1,15,24]

If the experimental route ($(MeO)_3B$ decomposition–oxidation–nitrification) is modified by direct exposure of the boride type film to ammonia (in total 1600 L at 900 K) by omitting an intermediate oxidation step, the XPS and LEED

analysis (Figure 2e and Figure 3e) still reveals the formation of boron nitride, but also the original boride type species and carbon can be detected by XPS (Figure 2e, C1s 284.4 eV, B1s 190.6 eV, and 188.4 eV, N1s 398.3 eV; Rh:C:B:N = 0.73:0.11:0.098:0.06).

The corresponding LEED profile (Figure 3e) reveals an ordering of the newly formed BN film. Since the (10) spot now displays additional intensity at larger transfer of momentum due to additional contributions from the BN lattice, that is, $(10) = (10)_{Rh} + (10)_{BN}$ (Figure 3e, inset). This LEED profile exhibits no additional superstructure spots (cf. profile Figure 3d) and is very similar to those obtained directly after precursor decay (Figure 3b). Therefore, the actual surface structure is expected to represent an admixture of the boride-type layer and a BN film. However, the onset of BN formation and the absence of any superstructure spots (Figure 3e) indicate that the average size of ordered BN domains is smaller (or at least not much larger) than the size of the superstructure cell (ca. 3.2 nm). This experiment indicates that the boride-type film can be directly converted into a BN containing film by reaction with ammonia, but the reaction proceeds much slower than for the oxidation–nitrification route and even stops.

The unexpected observations (no significant oxygen and carbon deposition during CVD of $(MeO)_3B$ and formation of a boride-type film) can formally be interpreted by a dehydroboration reaction (Scheme 1) leading to an elimination of a keto species (formaldehyde, CH_2O) and the intermediate formation of boron hydrides. Volatile cleavage- and decomposition products (generalized as $C_xH_yO_z$ type species) are considered responsible for the simultaneous removal of most of the carbon and oxygen. From a boron hydride intermediate the incorporation of boron into the substrate is feasible as observed in the experiment. Any other decay mechanism

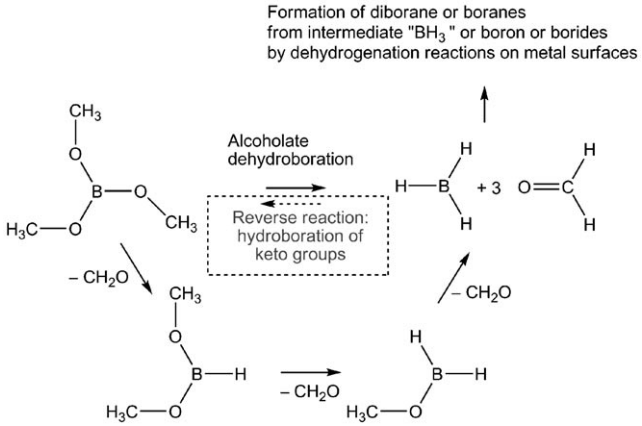

Scheme 1. Formal decay of $(MeO)_3B$. The reaction sequence derived from an interpretation of the observed formation of a boride-type film suggests a preferred fragmentation of the precursor into species containing carbon and oxygen and species containing boron. This reaction is, for example, compatible with a reversed hydroboration reaction ("alcoholate dehydrometalation reaction").

involving retention of a boron-oxygen bond, which formally might be expected from the bond energies, would lead to traceable formation of boron–oxygen species on the substrate surface. However, although the stability of sp^2-type B–O bonds would actually imply that precursors containing such bonds serve as sources for boron–oxygen-containing solids rather than boron or boride-type films, it was possible to directly incorporate boron into a Rh substrate by CVD of $(MeO)_3B$, a fully oxidized boron species, at quite low temperatures (900 K), thus indicating an unexpected decay of the precursor.

The presented experiments (summarized in Figure 5) reveal insight into the elementary steps of a chemical route

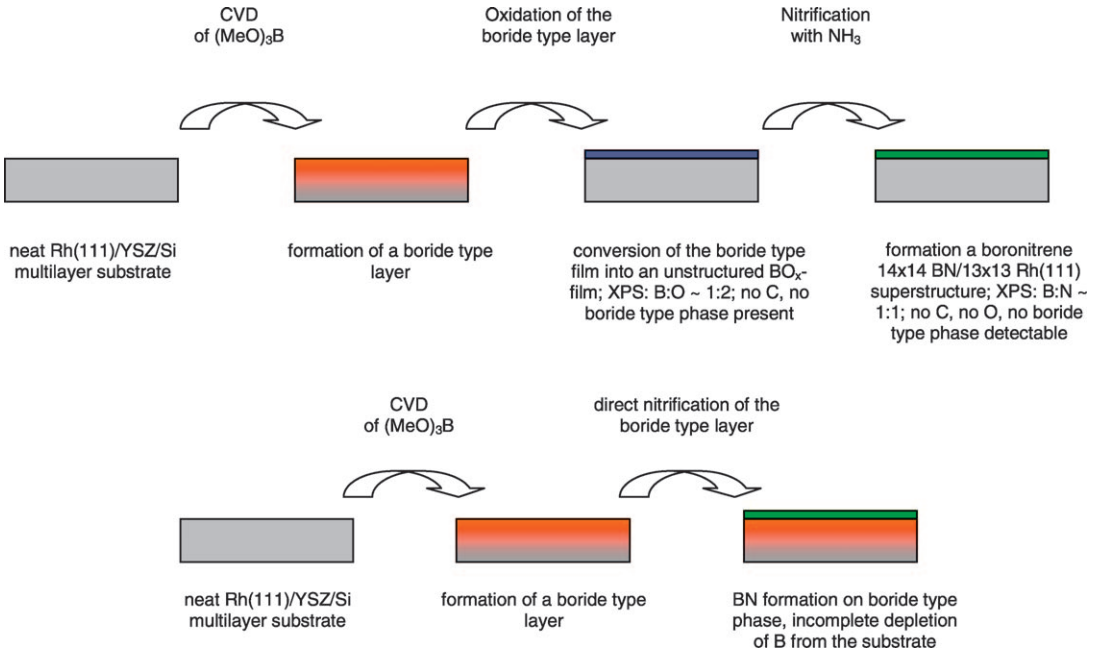

Figure 5. Summary of the reaction sequences: Formation of BN layers from $(MeO)_3B$ by surface-specific reactions with an oxidation step (top) and without (bottom).

to atomic layer deposition and growth for sp^2-type boron nitride phases. It is likely that changes in the conditions (e.g. higher precursor concentrations or variation of pressure and temperature) may alter the stoichiometries and structures of the resulting layers. Since carbon may also be deposited from the cleavage products of the precursor, variations of the decomposition conditions may reveal information up to what extent transition-metal carborides MC_xB_y (or carboboronitrides $MC_xB_yN_z$) are accessible.

The observed reaction sequence implies a decay for $(MeO)_3B$ which formally can be interpreted as a dehydroboration of a carbonyl function (Scheme 1). Similar reactions are feasible for metals of appropriate acidity linked to an alkoxide with α-CH functionality and can be considered as an "alcoholate dehydrometalation reactions" via intermediate metal hydrides and the keto species as formally described in Scheme 2.

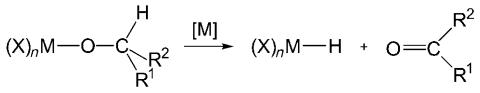

Scheme 2. Alcoholate dehydrometalation reactions. R^1, R^2 = aryl, alkyl or R^1 = aryl, alkyl and R^2 = H; X = any type of substituent; M = any type of acidic metal, for example, B, Al, Ga, Si, Ge, lanthanides, transition metals.

In the present experiment, the transition metal serves as a substrate for the generation of a boride-type layer and may also act catalytically for lowering the activation energy of the precursor decay. Currently this type of dehydrometalation reaction is being explored with other acidic metals. Also, boride, carboride, and (transition)metal carbide-boride-nitride layers of a general composition $MB_xC_yN_z$ might be accessible by this method (e.g. with Ti, Zr, Hf, Cr, Mo, W, and related metals).

Experimental Section

Methods: The experiments were performed with a modified VG ESCA MkII spectrometer designed for electron spectroscopy using angular resolution and described in detail in Refs. [28,29] The errors for the relative stoichiometries obtained by XPS are within 10% of the reported values.

Substrate pretreatment and preparation of the films: The Rh multilayer substrate[23] was cleaned through cycles of argon ion etching and annealing. $(MeO)_3B$ was used as a CVD precursor for the preparation of the layers grown by similar procedures as described in Ref. [24] at a substrate temperature of 800 K. $(MeO)_3B$ (distilled over CaH_2/$NaBH_4$ and free of detectable amounts of water, alcohol, boronic acids, and boroxines as shown by ^1H and ^{11}B NMR spectroscopy) was let into the preparation chamber through a leak valve, with the nozzle placed close to the surface of the substrate. Oxidation experiments were carried out using oxygen 5.8; nitrification was performed with ammonia 3.8. These gases were added directly onto the substrate through a leak valve.

Received: May 4, 2010
Revised: September 10, 2010
Published online: March 18, 2011

Keywords: boron · chemical vapor deposition · monolayers · nitrides · surface analysis

[1] H. Sachdev, F. Müller, S. Hüfner, *Diamond Relat. Mater.* **2010**, *19*, 1027 – 1033.
[2] H. Sachdev, New aspects in Borazine Chemistry, unpublished results, presented at the conference "Chemiedozententagung" Giessen, Germany, 8 – 10.3.2010.
[3] H. Sachdev, F. Müller, S. Hüfner, unpublished results (comparison of the CVD of borazines on Ag(111)).
[4] M. Corso, W. Auwärter, M. Muntwiler, A. Tamai, T. Greber, J. Osterwalder, *Science* **2004**, *303*, 217 – 220.
[5] R. Laskowski, P. Blaha, T. Gallauner, K. Schwarz, *Phys. Rev. Lett.* **2007**, *98*, 106802.
[6] H. Dil, J. Lobo-Checa, R. Laskowski, P. Blaha, S. Berner, J. Osterwalder, T. Greber, *Science* **2008**, *319*, 1824 – 1826.
[7] S. Berner, M. Corso, R. Widmer, O. Groening, R. Laskowski, P. Blaha, K. Schwarz, A. Goriachko, H. Over, S. Gsell, M. Schreck, H. Sachdev, T. Greber, J. Osterwalder, *Angew. Chem.* **2007**, *119*, 5207 – 5211; *Angew. Chem. Int. Ed.* **2007**, *46*, 5115 – 5119.
[8] R. Widmer, D. Passerone, T. Mattle, H. Sachdev, O. Gröning, *Nanoscale* **2010**, *2*, 502 – 508.
[9] A. J. Pollard, E. W. Perkins, N. A. Smith, G. Goretzki, A. G. Phillips, S. Argent, H. Sachdev, F. Müller, S. Hüfner, S. Gsell, M. Fischer, B. Strizker, M. Schreck, N. R. Champness, P. H. Beton, *Angew. Chem.* **2010**, *122*, 1838 – 1843; *Angew. Chem. Int. Ed.* **2010**, *49*, 1794 – 1799.
[10] A. Nagashima, N. Tejima, Y. Gamou, T. Kawai, C. Oshima, *Surf. Sci.* **1996**, *357–358*, 307 – 311.
[11] W. Auwärter, T. J. Kreutz, T. Greber, J. Osterwalder, *Surf. Sci.* **1999**, *429*, 229 – 236.
[12] W. Auwärter, H. U. Suter, H. Sachdev, T. Greber, *Chem. Mater.* **2004**, *16*, 343 – 345.
[13] F. Müller, K. Stöwe, H. Sachdev, *Chem. Mater.* **2005**, *17*, 3464 – 3467.
[14] W. Auwärter, M. Muntwiler, J. Osterwalder, T. Greber, *Surf. Sci.* **2003**, *545*, L735.
[15] F. Müller, S. Hüfner, H. Sachdev, *Surf. Sci.* **2009**, *603*, 425 – 432.
[16] K. Watanabe, T. Taniguchi, H. Kanda, *Nat. Mater.* **2004**, *3*, 404 – 409.
[17] J. Yu, S. Matsumoto, *Diamond Relat. Mater.* **2003**, *12*, 1539 – 1543.
[18] H. Sachdev, M. Strauß, *Diamond Relat. Mater.* **2000**, *9*, 614 – 619.
[19] H. Sachdev, *Diamond Relat. Mater.* **2001**, *10*, 1390 – 1397.
[20] T. Taniguchi, K. Watanabe, S. Koizumi, *Phys. Status Solidi A* **2004**, *201*, 2573 – 2577.
[21] Y. Kubota, K. Watanabe, T. Taniguchi, *Jpn. J. Appl. Phys.* **2007**, *46*, 311 – 314.
[22] T. Taniguchi, T. Teraji, S. Koizumi, K. Watanabe, S. Yamaoka, *Jpn. J. Appl. Phys.* **2002**, *41*, L109 – L111.
[23] S. Gsell, M. Fischer, M. Schreck, B. Stritzker, *J. Cryst. Growth* **2009**, *311*, 3731 – 3736.
[24] F. Müller, S. Hüfner, H. Sachdev, S. Gsell, M. Schreck, *Phys. Rev. B* **2010**, *82*, 075405.
[25] J. Kiss, K. Révész, F. Solymosi, *Appl. Surf. Sci.* **1989**, *37*, 95 – 110.
[26] R. W. Mooney, A. J. E. Welch, *Acta Crystallogr.* **1954**, *7*, 49 – 53.
[27] C. Kapfenberger, K. Hofmann, B. Albert, *Solid State Sci.* **2003**, *5*, 925 – 930.
[28] F. Müller, P. Steiner, T. Straub, D. Reinicke, S. Palm, R. de Masi, S. Hüfner, *Surf. Sci.* **1999**, *442*, 485 – 497.
[29] F. Müller, R. de Masi, P. Steiner, D. Reinicke, M Stadtfeld, S. Hüfner, *Surf. Sci.* **2000**, *459*, 161 – 172.

